Proposal of Nonlinear Friction Compensation Approach for a Ball-Screw-Driven Stage in Zero-Speed Region including Non-Velocity-Reversal Motion

Hongzhong Zhu and Hiroshi Fujimoto
Department of Electrical Engineering, The University of Tokyo
5-1-5 Kashiwanoha, Kashiwa, Chiba, 277-8561, Japan
Email: zhu@hflab.k.u-tokyo.ac.jp, fujimoto@k.u-tokyo.ac.jp

***Abstract*—This paper presents a heuristic friction compensation approach for handling the springlike friction behaviors of a ball-screw-driven stage in zero-speed region. The friction compensation for the motion that the stage is decelerated to stop and then accelerated in the same direction, which is also referred to as non-velocity-reversal motion, is discussed in detail. As the elastic energy stored in mechanical components may not be completely released during non-velocity-reversal motion, the conventional compensation approaches may not work well. Therefore, some other sophisticated friction compensation approaches become necessary for this kind of motion. In this study, a velocity pattern recognition algorithm is presented as the first step to classify the velocity patterns in zero-speed crossing region. Then, sinc function is exploited to model the nonlinear springlike friction of the ball-screw-driven stage. It is proved that the friction can be properly compensated for both the reversal motion and non-reversal motion. Experiments are performed to verify the proposed approach and it is demonstrated that the control performance is significantly improved.**

I. Introduction

The demand for high-precision stages has received great attention in recent years due to the progress of nano-technology. Systems to provide long-range and high-precision performance for positioning, tracking and contouring actions are increasingly required. Among these systems, the ball-screw-driven systems have been widely used in many applications for their high efficiency and low cost [1], [2], [3], [4]. However, due to the nonlinearity of the friction which originates at elastic deformation of the mechanical components, the control performance may be significantly degraded at low speed motion, especially in the zero-speed region [5], [6], [7].

In order to compensate nonlinear friction, many researchers focused on obtaining precise friction models. Among them, Dahl model and LuGre model are proposed to describe the spring-like behavior in stiction [8], [9]. Hsieh and Pan proposed a novel model combining two major characteristics of static friction: the hysteresis and the plasticity [10]. Swevers *et al.* presented a complete and accurate model that can describe the hysteresis characteristics of the friction [11]. The models are so complex that not only the identification of the parameters but also the implementation to the real systems are hard. In order to take more priority over the ease of implementation, a heuristic friction model, which is also referred to as the Generalized Maxwell-Slip Model (GMS), was proposed in [12]. In the model, the physical meanings of the parameters are clear. However, the identification of the model is also a time-consuming work. Besides, Almost all of the proposed approaches only considered the compensation for reversal motion, which may not enough for the cases of complex machining. For instance, in the case of non-reversal motion where the stage is decelerated to zero velocity and then accelerated in the same direction, the elastic energy stored in mechanical components may not be completely released. In this case, the torque compensation strategy are different with the case of reversal motion.

Another well known method for suppressing nonlinear friction is disturbance observer [13], [14], [15]. The method can significantly improve the control performance. However, due to the phase lag of the introduced low-pass filter and the inaccuracy of velocity signal, nonlinear friction cannot be completely reduced in zero-speed region. Therefore, disturbance observer method and friction compensator coexist in many proposed approaches [6], [15], [16]. This structure is also applied in this study.

For tracking control purposes, a simple model to describe the nonlinear static friction is preferred for the ease of use. Motivated by this perspective, the purposes of this work are to propose a model whose parameters can be easily identified, and to propose an efficient friction compensation approach which can not only cope with the reversal motion but also the non-reversal motion. More concretely, a velocity pattern classification in zero-speed crossing region is presented as the first step. Based on velocity patterns, a heuristic approach of friction compensation for our experimental ball-screw-driven stage is proposed based on sinc function. It is illustrated that the rolling friction characteristics can be properly modelled by sinc function. Finally, a torque compensation algorithm for non-reversal motion is developed based on Newton iteration method.

The remainder of this study is organized as follows. Section

TABLE I
PARAMETERS OF THE STAGE IN X-AXIS DIRECTION

motor inertia moment J_m	2.3×10^{-3} kgm^2
motor viscosity coefficient B_m	1.1772 Nms/rad
length of ball screw L_b	1.169 m
mass of ball screw M_b	9.3526 kg
inertia moment of ball screw J_b	1.0052×10^{-3} kgm^2
viscosity coefficient of ball screw B_b	5.0×10^{-2} Nms/rad
lead of ball screw L_p	1.2×10^{-2} m
mass of table M_t	273.0 kg
viscosity coefficient of linear guide C_t	1.0×10^4 Ns/m

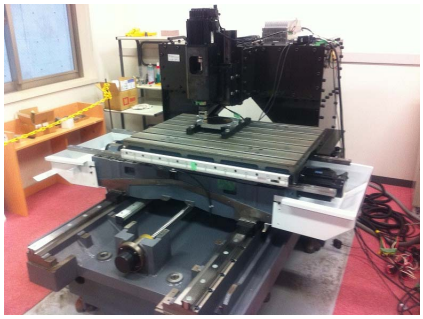

Fig. 1. Ball-screw-driven X-Y stage.

II described the experimental setup. Section III presents the algorithm to classify the velocity patterns in zero-speed region. Then, a nonlinear friction compensation approach based on sinc function is proposed in Section IV. Experiments are performed to show the effectiveness of the proposed approach in Section V. Finally, the conclusion is summarized in Section VI.

II. EXPERIMENTAL BALL-SCREW-DRIVEN STAGE SYSTEM

A. Ball-screw-driven stage

Fig. 1 shows the overview of the experimental X–Y ball-screw stage. Each ball screw is directly connected with the shaft of the servo motor through coupling. The servo motor is equipped with an absolute encoder whose resolution is 2^{20} pulse/rev. Linear scales with a resolution of 100 nm are applied to measure the X,Y-axis positions of the stage. Table. I shows the parameters of the stage in X-axis direction. The stage can be model as a two-inertia system whose block diagram is shown in Fig. 2. Here,

ω rotation velocity, $[\mathrm{rad/s}]$,
θ rotation angular, $[\mathrm{rad}]$,
f_r torque caused by rolling friction, $[\mathrm{N \cdot m}]$,
v velocity of stage, $[\mathrm{m/s}]$,
x_t position of stage, $[\mathrm{m}]$,
f_l nonlinear friction caused by linear guide, $[\mathrm{N}]$,
T_m motor torque, $[\mathrm{N \cdot m}]$,
J_r rotative inertia, $[\mathrm{kgm^2}]$,
B_r viscosity coefficient in rotative direction, $[\mathrm{Nms/rad}]$,
R motion translation ratio, $\frac{L_p}{2\pi}$,
K_t torque constant, $[\mathrm{Nm/A}]$.

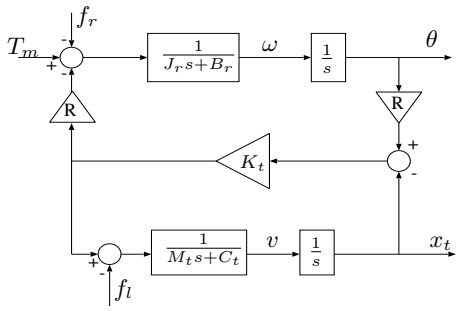

Fig. 2. Block diagram of the system.

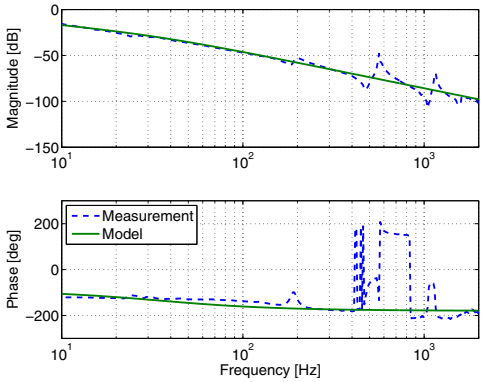

Fig. 3. Frequency response of stage from the current input to motor position θ.

The rigid-body model of the stage is expressed as follows:

$$P_n(s) := \frac{K_t}{Js^2 + Bs}, \tag{1}$$

where $J := J_r + M_t R^2$ is the nominal inertia and $B := B_r + C_t R^2$ is the nominal viscosity. Fig. 3 shows the frequency response of the experimental device, and the fitted model is shown by the solid line.

The rolling friction characteristics of the stage is shown in Fig. 4. It can be observed that the spring-like phenomenon appears at the presliding region $[0,\ 10]\mu\mathrm{m}$.

B. Controller design

The block diagram of control system is shown in Fig. 5. The feedforward controller is designed as the stable inverse system of the nominal plant via Perfect Tracking Control (PTC) method [17]. The perfect tracking at every sampling instant

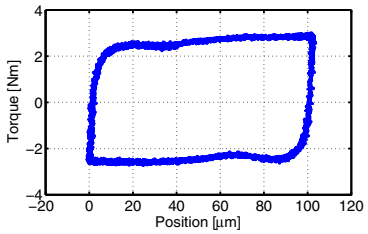

Fig. 4. Rolling friction of the experimental stage.

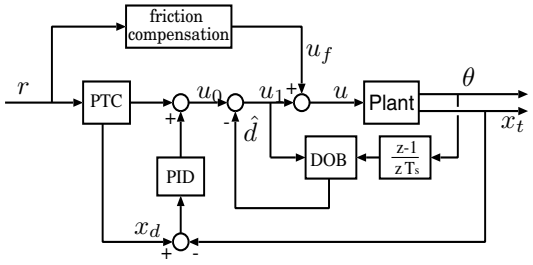

Fig. 5. Block diagram of control system with two-degree-of-freedom controller, an inverse-model-based disturbance observer and feedforward friction compensation.

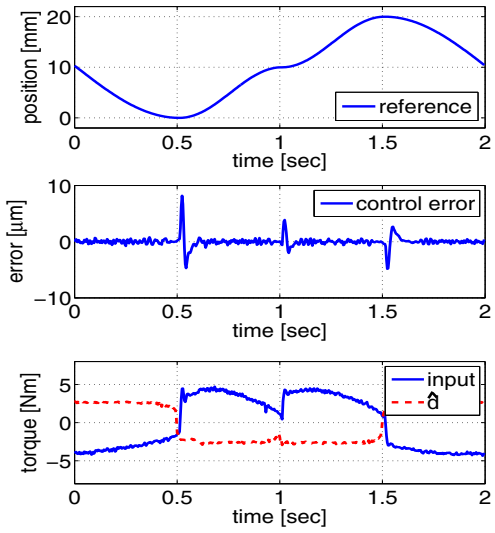

Fig. 6. Experimental results without friction compensation. The upper graph is the reference, the middle graph shows the position tracking error, and the lower graph shows the control input and estimated disturbance.

can be theoretically guaranteed. A PID compensator is applied as the feedback controller, and the resulting bandwidth of the closed loop is 20 Hz. An inverse-model-based disturbance observer (DOB) is designed using the motor velocity information [18]. A 1^{st}-order low-pass filter is designed for the disturbance observer whose bandwidth is 80 Hz. Feedforward friction compensation is considered in this study. DSP(TMS320C6713, 225MHz) is used as the processor to implement the controller. The PID compensator, DOB and friction compensation are discretized by 0.5 ms. The sampling period of the feedforward controller is 1 ms.

Without friction compensation, control performance is significantly degraded in zero-speed region. An experimental result is shown in Fig. 6. It is observed that the position tracking error is degraded in both the velocity-reversal region and non-reversal region. The compensation for the reversal case has already been actively studied in the literature. However, the study for the non-reversal case is rare as far as the authors know. In the following sections, a heuristic method based on sinc function is examined to cope with the situations.

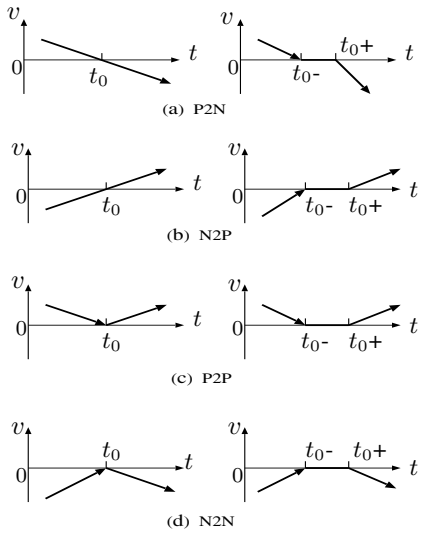

Fig. 7. Classification of velocity patterns in the rolling region.

III. Velocity Patterns Classification and Sinc-Function-Based Friction Compensation

A. Velocity patterns classification

In this subsection, an algorithm to classify the velocity patterns in zero-speed region is studied. For simplicity, the trajectory reference is assumed to be known and twice differentiable. In practical situations, this assumption can be generally satisfied.

For the ease of analysis, we denote $r(t)$, $v(t)$ and $a(t)$ as the desired trajectory, velocity and acceleration, respectively. Their discretized signals are denoted by r_k, v_k and a_k, where k is the discrete-time index. p_k is defined to label the sign of the acceleration a_k by

$$p_k = \begin{cases} 1, & a_k > 0 \\ -1, & a_k < 0 \\ p_{k-1}, & a_k = 0. \end{cases} \tag{2}$$

Usually, velocity changes in zero-speed region have four patterns shown as follows according to the change of the sign of $v(t)$:

- P2N: Positive $\Rightarrow$ zero $\Rightarrow$ negative;
- N2P: Negative $\Rightarrow$ zero $\Rightarrow$ positive;
- P2P: Positive $\Rightarrow$ zero $\Rightarrow$ positive;
- N2N: Negative $\Rightarrow$ zero $\Rightarrow$ negative.

Fig. 7 illustrates the velocity patterns in zero-speed region. The algorithm to classify these patterns in discrete time is shown in Fig. 8. Here, ϵ is a threshold set to be a little larger than the minimum variation in a sampling period. In the next section, a heuristic method for friction compensation is proposed based on the velocity patterns.

B. Sinc-function-based friction compensation

Many friction models proposed in the literature are complex and hard to robustly cope with the environment-affected friction. Additionally, an ultra-precision model of friction is

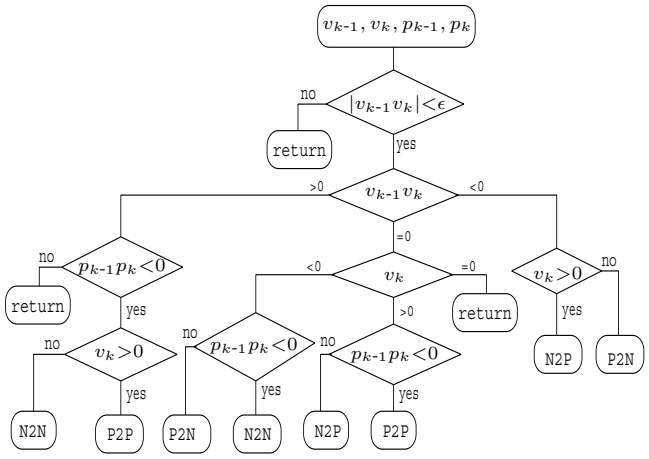

Fig. 8. Algorithm to Classify the velocity patterns in the rolling region.

not always necessary for robust control purpose. Therefore, a simple friction model which can be easily tuned is of interest. Motivated by this view and taken the characteristics of ball screw into account, the sinc function is exploited in this paper.

Sinc function is defined by

$$y(x) = \mathrm{sinc}(x) := \begin{cases} \frac{\sin(x)}{x}, & x \neq 0 \\ 1, & x = 0 \end{cases} . \tag{3}$$

The Fourier transform of the function is a rectangular function expressed by

$$Y(f) = \begin{cases} 0, & |f| > \frac{\pi}{2} \\ \frac{1}{2}, & |f| = \frac{\pi}{2} \\ 1, & |f| < \frac{\pi}{2}. \end{cases} \tag{4}$$

Note that the sinc function is an ideal low-pass filter. In the following, a novel friction compensation for ball-screw stage is presented.

In the N2P case, sinc function applied to fit the rolling friction is expressed by

$$u_{f_a} = \begin{cases} -F_0, & x < 0 \\ 2F_0 \frac{\sin\left(\pi\sqrt{\frac{x}{x_s}}-\pi\right)}{\pi\sqrt{\frac{x}{x_s}}-\pi} - F_0, & 0 \leq x < x_s \\ F_0, & x \geq x_s \end{cases} , \tag{5}$$

where x is the displacement of position from the reverse point of N2P case, x_s is the length of the presliding region, and F_0 can be regarded as the Coulomb friction. For the motion in the negative direction, a similar formula can be obtained. Fig. 9 illustrates the rolling friction characteristic. The comparison of the real rolling friction and the sinc-function-based model is shown in Fig. 10, where $x_s = 10\,\mu$m and $F_0 = 2.431\,$Nm. It can be observed that an accurate fitting is achieved.

In the case of reversal motion, the elastic deformation of mechanical components comes to the equilibrium point before they are excited again. The rolling friction varies between $\pm F_0$, and therefore has the potential to be well compensated by properly designed friction models. However, if this is not the case, such as N2N and P2P, the excited elastic energy is

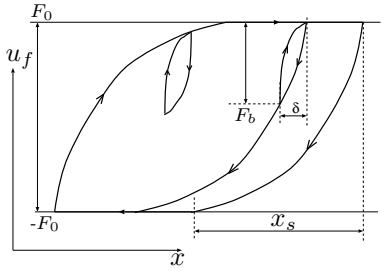

Fig. 9. Rolling friction characteristic.

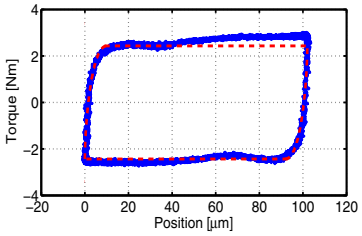

Fig. 10. Comparison of the real rolling friction and sinc function based model.

not fully released, thus the compensation becomes complex. In the following, sinc function is utilized to perform the compensation. For simplicity, the P2P case is used for analysis.

As the velocity is decelerated to zero, torque is gradually reduced due to the 2-dof controller and the disturbance observer. In this step, the excited elastic energy is partly released so that the magnitude of friction also reduces. The experimental result is shown in Fig. 6. When the acceleration motion starts, the elastic deformation need to be re-established.

Suppose that the magnitude of friction is reduced to F_b until the acceleration starts, the released displacement δ can be calculated according to

$$-2F_0 \frac{\sin\left(\pi\sqrt{\frac{\delta}{x_s}}-\pi\right)}{\pi\sqrt{\frac{\delta}{x_s}}-\pi} + F_0 = F_b. \tag{6}$$

Newton iteration method can be applied to solve the δ. The details are given in Appendix. Fig. 9 demonstrates this explanation. When (6) is solved, δ is set as the new length of presliding region. The compensation based on sinc function is given by

$$u_{f_b} = \begin{cases} 0, & y \leq 0 \\ (F_0 - F_b)\frac{\sin\left(\pi\sqrt{\frac{y}{\delta}}-\pi\right)}{\pi\sqrt{\frac{y}{\delta}}-\pi}, & 0 < y < \delta \end{cases} , \tag{7}$$

where y is the displacement of position from the point of zero velocity. A similar compensation method can be obtained in the case of N2N pattern.

The friction compensation is realized by $u_f = u_{f_a} + u_{f_b}$, where u_{f_a} is the compensation value for reversal motion and u_{f_b} is the compensation value for non-reversal motion. Fig. 11 shows the strategy of friction compensation. In the real situation, u_{f_b} need to be reduced to zero slowly, or else the

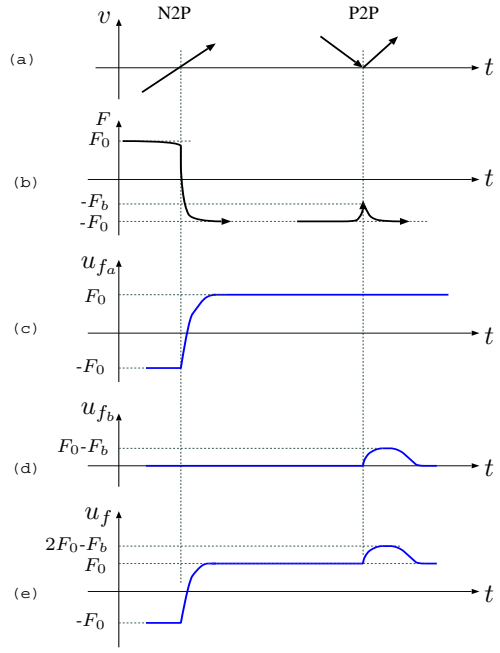

Fig. 11. Illustration of the strategy of the friction compensation. (a) shows the velocity patterns, (b) shows the changing trend of friction, (c), (d) demonstrate the u_{f_a} and u_{f_b}, respectively, and u_f is shown in (e).

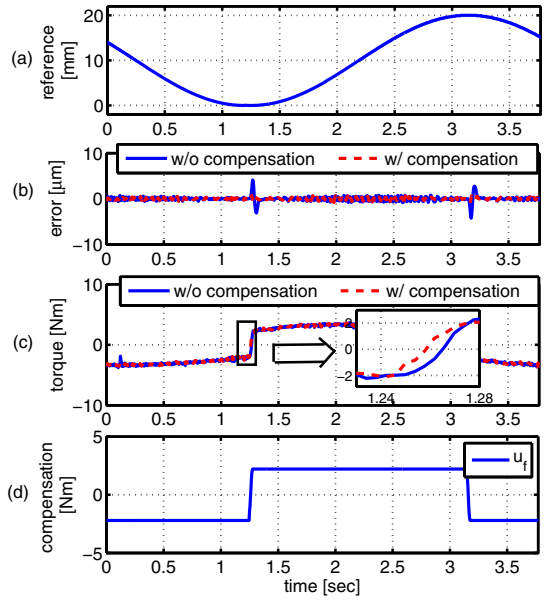

Fig. 12. Experimental results in the case of $v_{\max} = 1\,\mathrm{m/min}$.

compensation value will be accumulated and increases continuously if the following motion is still a non-reversal motion. In order to make the compensation smoothly without raising harmonic resonance to the system, another sinc function is exploited to reduce u_{f_b} to zero. Therefore, the compensation for non-reversal case is given by

$$u_{f_b} = \begin{cases} 0, & y \le 0 \\ (F_0 - F_b)\,\dfrac{\sin\left(\pi\sqrt{\frac{y}{\delta}} - \pi\right)}{\pi\sqrt{\frac{y}{\delta}} - \pi}, & 0 \le y < \delta \\ (F_0 - F_b)\,\dfrac{\sin\left(\pi\sqrt{\frac{y-\delta}{x_m}}\right)}{\pi\sqrt{\frac{y-\delta}{x_m}}}, & y \ge \delta \end{cases} \tag{8}$$

x_m should be set sufficiently large to slowly reduce u_{f_b} to zero. In general, setting of x_m need to take the bandwidth of DOB into account in order to let DOB respond quick enough to compensate the reduced torque. The compensation approach is shown as the solid line in Fig. 11(d).

IV. Experiments

In this section, the proposed friction compensation method is verified by experiments. Firstly, a sine wave with the magnitude of $10\mathrm{mm}$ is implemented as the trajectory reference to evaluate the compensation performance of the reversal motion. Two cases that the maximum feed rates are $1\,\mathrm{m/min}$ and $5\,\mathrm{m/min}$ are considered. Fig. 12 and Fig. 13 show their experimental results. In the figures, (a)s show the reference signal. The comparison of position tracking errors without compensation and with compensation is shown in (b)s. It is observed that the compensation performance was significantly improved by the proposed friction compensation approach. The maximum tracking error is improved from $4.2\,\mu\mathrm{m}$ to $0.92\,\mu\mathrm{m}$ for the first case, and improved from $8.2\,\mu\mathrm{m}$ to $1.98\,\mu\mathrm{m}$ for the second case. The control inputs are shown in (c)s and the compensation torques are shown in (d)s. Thanks to the compensation, the control inputs can respond faster to reduce the effects of rolling friction.

In addition, the compensation effectiveness for the P2P pattern is also evaluated. The trajectory reference is set as the same with the one in Fig. 6. The experimental results are shown in Fig. 14. Compared with the results shown in Fig. 6, we can see that with compensation, the tracking error can be significantly improved in the P2P case. The tracking error at the P2P region is improved from $3.86\,\mu\mathrm{m}$ to $1.55\,\mu\mathrm{m}$. Therefore, the effectiveness of the proposed method is verified.

V. Conclusion

In this study, a novel friction compensation method based on velocity pattern recognition and sinc function is proposed. Compared to conventional friction models, the proposed compensation approach can cope with both the reversal motion and non-reversal motion. It also has an advantage that the two parameters in the friction model have clear physical meanings that can be easily identified. The proposed approach is also verified by experiments in combination with an inverse-model-based disturbance observer. It is demonstrated that the position tracking performance can be significantly improved in the zero-speed crossing region.

Appendix

The approach for numerically solving the equation (6): Assume $-F_0 < F_b < F_0$ without loss of generality, and

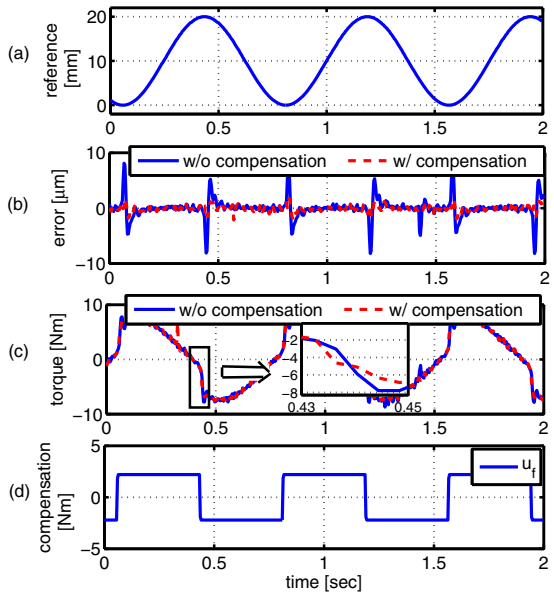

Fig. 13. Experimental results in the case of $v_{\max} = 5\,\mathrm{m/min}$.

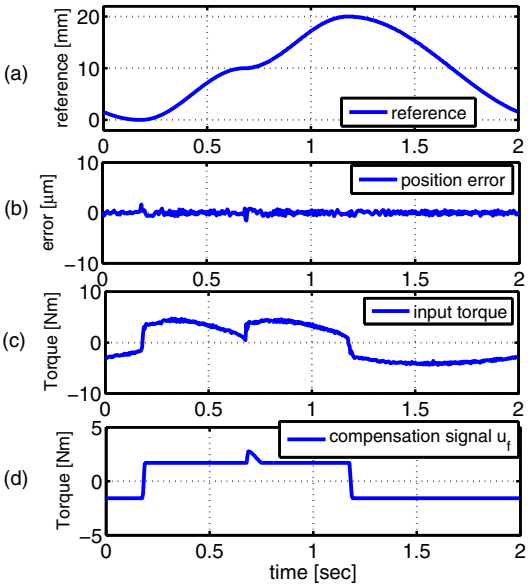

Fig. 14. Experimental results when the reference is irregular.

denote

$$M := \frac{F_0 - F_b}{2F_0}, \tag{9}$$

$$q := \pi - \pi\sqrt{\frac{\delta}{x_s}} \tag{10}$$

for the convenience of calculation. It can be obtained that $0 < q < \pi$ since $0 < \delta < x_s$. The equation (6) can be rewritten by

$$\sin q = Mq, \quad 0 < q < \pi. \tag{11}$$

Define $g(q) = Mq - \sin q$, the equation $g(q) = 0$ can be efficiently solved by mathematical iteration approach, such as Newton iteration method, since $g(q)$ is convex in $0 < q < \pi$ ($g'' > 0$). If q is calculated, δ can be solved according to (10).

ACKNOWLEDGE

This work was supported in part by the MORI SEIKI Co. Ltd.. The authors gratefully acknowledge valuable suggestions from Shinji ISHII, Kouji YAMAMOTO and Yuki TERADA from the MORI SEIKI Co. Ltd..

REFERENCES

[1] F. Huo, and A.-N. Poo, "Precision Contouring Control of Machine Tools", *Int. J. Adv. Manuf. Technol.*, Vol. 64, pp. 319–333, 2013.

[2] Y. Altintas, A. Verl, C. Brecher, L. Uriarte, and G. Pritschow, "Machine Tool Feed Drives", *Manufacturing Technology*, Vol. 60, pp. 779–796, 2011.

[3] C.L. Chen, M.J. Jang, and K.C. Lin, "Modeling and High-Precision Control of a Ball-Screw-Driven Stage", *Precision Engineering*, Vol. 28, pp. 483–495, 2004.

[4] M. Iwasaki, K. Seki, and Y. Maeda, "High-Precision Motion Control Techniques–A Promising Approach to Improving Motion Performance", *IEEE Trans. Ind. Electron. Magazine*, Vol. 6, No. 1, pp. 32–40, 2012.

[5] M. Iwasaki, M. Miyaji, N. Matsui, "High-Precision Contouring Control of Table Drive System in Machine Tools Using Lost Motion Compensation", *IEEJ Trans. IA*, Vol. 125, No. 6, pp. 616–622, 2005.

[6] H. S. Lee and M. Tomizuka, "Robust Motion Controller Design for High-Accuracy Positioning Systems", *IEEE Trans. Indust. Electr.* , Vol. 43, No. 1, pp. 48–55, Feb. 1996.

[7] S. Fukada, B. Fang, and A. Shigeno, "Experimental Analysis and Simulation of Nonlinear Microscopic Behavior of Ball Screw Mechanism for Ultra-Precision Positioning", *Precision Engineering*, Vol. 35, pp. 650–668, 2011.

[8] P. Dahl, "A solid friction model", Aerospace Corp., El Segundo, CA, Tech. Rep. TOR-0158(3107-18), 1968.

[9] C. Canudas de Wit, H. Olsson, K. Astrom and P. Lischinsky, "A new model for control of systems with friction", *IEEE Trans. Autom. Control*, Vol. 40, No. 5, pp. 419–425, 1995.

[10] C. Hsieh, and Y.C. Pan, "Dynamic Behavior and Modelling of the Presliding Static Friction", *Wear*, Vol. 242, pp. 1-17, 2000.

[11] J. Swevers, F. Al-Bender, C. G. Ganseman, and T. Prajogo, "An integrated friction model structure with improved presliding behavior for accurate friction compensation", *IEEE Trans. Automat. Contr.*, Vol. 45, pp. 675–686, Apr. 2000.

[12] F. Al-Bender, V. Lampaert and J. Swevers, "The Generalized Maxwell-Slip Model: A Novel Model for Friction Simulation and Compensation", *IEEE Trans. Autom. Control*, Vol. 50, No. 11, pp. 1883–1887, 2005.

[13] S. Sakai and Y. Hori, "Ultra-low Speed Control of Servomotor using Low Resolution Rotary Encoder", in *Proc. IECON 21st int. Conf. Ind. Electron.* , Orlando, FL, Vol. 1, pp. 615–620, 1995.

[14] W.S. Huang, C.W. Liu, P.L. Hsu, and S.S. Yeh, "Precision Control and Compensation of Servomotors and Machine Tools via the Disturbance Observer", in *IEEE Trans. Ind. Electro.* , Vol. 57, No. 1, pp. 420–429, 2010.

[15] Y. Maeda, and M. Iwasaki, "Analytical Examinations and Compensation for Slow Settling Response in Precise Positioning Based on Rolling Friction Model", *Advanced Motion control* , pp. 24–29, Nagaoka, Mar. 2010.

[16] Z. Jamaludin, H. V. Brussel, and J. Swevers, Friction Compensation of an XY Feed Table Using Friction-Model-Based Feedforward and an Inverse-Model-Based Disturbance Observer, *IEEE Trans. Ind. Electron.* , Vol. 56, No. 10, pp. 3848–3853, 2009.

[17] H. Fujimoto, Y. Hori, and A. Kawamura, "Perfect Tracking Control based on Multirate Feedforward Control with Generalized Sampling Periods", *IEEE Trans. Ind. Electron.*, Vol. 48, No. 3, pp. 636–644, 2001.

[18] T. Umeno and Y. Hori, Robust Speed Control of DC Servomotors Using Modern Two Degree-of-Freedom Control Design, *IEEE Trans. Indust. Electr.* , Vol. 38, No. 5, pp. 363–368, Oct. 1991.